

PAPER • OPEN ACCESS

## Processing of AlCoCrFeNiTi high entropy alloy by atmospheric plasma spraying

To cite this article: M Löbel *et al* 2017 *IOP Conf. Ser.: Mater. Sci. Eng.* **181** 012015

View the [article online](#) for updates and enhancements.

### You may also like

- [Microstructural development in nanostructured AlCoCrFeNi-ZrO<sub>2</sub> high-entropy alloy composite prepared with mechanical alloying and spark plasma sintering methods](#)

M Ghanbariha, M Farvizi and T Ebadzadeh

- [Microstructure and mechanical properties of AlCoCrFeNi high entropy alloys produced by spark plasma sintering](#)

P F Zhou, D H Xiao, Z Wu et al.

- [Precipitation behavior of yttrium-rich nano-phases in AlCoCrFeNi<sub>2.4</sub>Y<sub>x</sub> high-entropy alloy](#)

Minghong Sha, Yanwen Zhou, Ning Wang et al.

The advertisement features the ECS logo and the text "The Electrochemical Society" and "Advancing solid state & electrochemical science & technology". It also includes images of a robotic arm in a manufacturing setting and a woman looking at a colorful chart or graph.

**DISCOVER**  
how sustainability  
intersects with  
electrochemistry & solid  
state science research

# Processing of AlCoCrFeNiTi high entropy alloy by atmospheric plasma spraying

M Löbel<sup>1</sup>, T Lindner<sup>1</sup>, C Kohrt<sup>2</sup> and T Lampke<sup>1</sup>

<sup>1</sup>Institute of Materials Science and Engineering, Chemnitz University of Technology,  
09125 Chemnitz, Germany

<sup>2</sup>Rhein-Ruhr Beschichtungs-Service GmbH, 47495 Rheinberg, Germany

**Abstract.** High Entropy Alloys (HEA) are gaining increasing interest due to their unique combination of properties. Especially the combination of high mechanical strength and hardness with distinct ductility makes them attractive for numerous applications. One interesting alloy system that exhibits excellent properties in bulk state is AlCoCrFeNiTi. A high strength, wear resistance and high-temperature resistance are the necessary requirements for the application in surface engineering. The suitability of blended, mechanically ball milled and inert gas atomized feedstock powders for the development of atmospheric plasma sprayed (APS) coatings is investigated in this study. The ball milled and inert gas atomized powders were characterized regarding their particle morphology, phase composition, chemical composition and powder size distribution. The microstructure and phase composition of the thermal spray coatings produced with different feedstock materials was investigated and compared with the feedstock material. Furthermore, the Vickers hardness (HV) was measured and the wear behavior under different tribological conditions was tested in ball-on-disk, oscillating wear and scratch tests. The results show that all produced feedstock materials and coatings exhibit a multiphase composition. The coatings produced with inert gas atomized feedstock material provide the best wear resistance and the highest degree of homogeneity.

## 1. Introduction

The term of HEA was introduced by Yeh et al. [1]. By definition, those new alloy systems are composed of at least five elements with a share of 5-35 at.% each. Usually the formation of brittle, intermetallic and complex phases is expected. Nevertheless, investigations have shown the formation of simple solid solutions with face centered cubic (FCC) and body centered cubic (BCC) structures due to the stabilization by high entropy effect. No intermetallic or complex phases were formed [1, 2]. At the same time, independent investigations were carried out by Cantor et al. [3], who proved that a single phase FCC structure forms in the equimolar alloy FeCrMnNiCo. Especially the usage of transition metals in the alloy system prevents the formation of intermetallic phases or complex compounds [1, 2]. However, structural investigations on most HEAs revealed a multiphase structure consisting of several phases [4]. Therefore the term compositionally complex alloys (CCA) was introduced for alloys, which are not composed of one single simple solid solution [5]. CCAs with a high share of Al and Ti are especially convenient to form lightweight HEAs due to their low density. An alloy system, which has already been investigated in bulk state, is AlCoCrFeNiTi. First investigations of Zhou et al. [6] revealed a dendritic structure consisting of two BCC solid solutions. Furthermore, high fracture strength of 2.58 GPa and plastic strain of 8.8 % were achieved in compression test. These properties were attributed to solid solution strengthening by Ti atoms [6].



Content from this work may be used under the terms of the [Creative Commons Attribution 3.0 licence](#). Any further distribution of this work must maintain attribution to the author(s) and the title of the work, journal citation and DOI.

Further investigations concentrated on the structure and influence of alloying elements, especially Ti and Al. Al showed strong influence on phase composition. For alloys with high Al content, mainly strong and brittle BCC phases were formed. Increasing the amount of Ti leads to strengthening by solid solution hardening and if added in high amounts to the formation of intermetallic phases [7-10]. A comparison of wear performance between the CCA system AlCoCrFeNiTi and conventional steels (SUJ2, SKH51) showed promising properties [10, 11]. So far, mainly bulk properties of HEAs and CCAs have been investigated. Only few investigations have been carried out to apply HEAs and CCAs by thermal spray technology. First investigations mainly focused on microstructural characterization and phase composition of coatings [12, 13]. However, some research has been carried out to investigate the wear resistance of thermal spray HEA coatings, revealing good wear resistance in comparison with conventional steel (SUJ2, SKD61) [14]. The focus of this study is the development of an AlCoCrFeNiTi coating for wear protection applications. Surface engineering by thermal spray processing enables a resource efficient use of material by functional division into surface and bulk parts. This is necessary for possible applications due to the application of expensive alloying elements in HEA/CCA alloy systems.

## 2. Experiments

### 2.1 Preparation and characterization of feedstock material

In this study different feedstock materials of the CCA system AlCoCrFeNiTi with equimolar composition are investigated. The first approach to supply feedstock for thermal spray processes was the production of a powder blend. Pure elemental powders were utilized, with the exception of Fe, which was added as pre-alloy FeCr13. The different powders were mixed in a tumbling mixer WAB Turbula. This powder blend was directly used as feedstock material for APS. Furthermore, the powder blend was used as a raw material for the production of alloyed powder with a homogeneous composition by high-energy ball milling (HEM) in a Zoz Simoloyer CM08 mill. Milling parameters are listed in table 1.

**Table 1.** Milling parameters for the production of alloyed powder by HEM utilizing a powder blend.

Ground material / powder mass	0.8 kg
Grinding medium	Steel balls (100Cr6 / Ø 5 mm)
Atmosphere	air
Ball to powder ratio (BPR)	10:1
Process control agent	Stearic Acid (SA)
Rotor speed	400-700 rpm cyclic)
Total milling time	14 h

Another attempt to produce homogeneous thermal spray powder was the application of inert gas atomization. In a first step, a homogeneous alloy was produced by melting elements under vacuum. Subsequently the alloy was atomized with Argon as inert process gas to avoid reactions. After atomization the powder was separated into several particle size fractions. The fraction with  $D_{90} < 100 \mu\text{m}$  was used for thermal spray.

All feedstock materials were investigated regarding their particle size distribution by laser diffraction analysis in a Cilas 930 device. For the milled and atomized powder, metallographic cross sections were prepared and investigated in the scanning electron microscope (SEM) Leo 1455VP to examine the structure, homogeneity and particle morphology. A backscattered electron detector (BSD) has been utilized to show material contrast. Furthermore, the chemical composition was investigated by energy dispersive X-Ray spectroscopy (EDX) with EDAX Genesis. Phase analysis was carried out by X-Ray diffraction (XRD) with a D8 Discover/Bruker AXS diffractometer using Co-K $\alpha$ -radiation.

## 2.2 Coating process and characterization

Prior to coating, steel flat substrates (S235) with a diameter of 40 mm were prepared by corundum blasting using corundum with grain size 425 – 600 µm, a pressure of 3.5 bar, a distance of 100 mm and angle of 60°. After ultrasonic cleaning in an ethanol bath, the substrates were coated with the APS system GTV-F6 to produce coatings with a thickness of approximately 200 µm. The parameters were adjusted according to optimize coating porosity and hardness. The resulting parameters for the different feedstock materials and are shown in table 2.

**Table 2.** APS parameters for applied feedstock materials.

	<b>Powder blend</b>	<b>HEM powder</b>	<b>Atomized powder</b>
Ar	38 l/min	38 l/min	54 l/min
H <sub>2</sub>	14 l/min	12.5 l/min	9 l/min
I	530 A	600 A	530 A
Powder feed rate	50 g/min	25 g/min	50 g/min
No. of layers	9	12	12
Spray distance	120 mm	120 mm	120 mm
Relative traverse speed	100 m/min	70 m/min	100 m/min
Spray path offset	4 mm	4 mm	4 mm

Cross sections of all coatings were prepared and examined by SEM to investigate the microstructure and phase composition. The chemical composition was investigated by EDX. In a next step, the Vickers hardness (HV) was measured in the cross sections with a Wilson Tukon 1102 device. Furthermore, the wear behavior under different tribological conditions was tested by ball-on-disk wear tests with a Tetra Basalt Tester, oscillating wear tests with a Wazau SVT 40 device and scratch tests with a CSM Revetest-RST device. The wear test parameters are shown in table 3.

**Table 3.** Wear test parameters for APS coatings.

<b>Ball-on-disk test</b>	<b>Oscillating wear test</b>	<b>Scratch test</b>	
force	20 N	mode	progressive
radius	5 mm	force	1-200 N
speed	96 rpm	speed	2.5 mm/min
cycles	15916	length	5 mm
Ø Al <sub>2</sub> O <sub>3</sub>	6 mm	tip	Truncated diamond cone, r: 200 µm
Ø Al <sub>2</sub> O <sub>3</sub>	10 mm		

Wear marks resulting from scratch and oscillating wear tests were investigated with a laser scanning microscope (LSM) Keyence VK-X200. Ball-on-disk wear tracks were analyzed with the stylus instrument Hommelwerke LV-50E. Furthermore, wear marks made by scratch tests were investigated with the digital microscope Keyence VHX-500.

## 3. Results and Discussions

### 3.1 Feedstock characterization

Metallographic cross sections of the milled and atomized powders were investigated and are shown in figure 1.

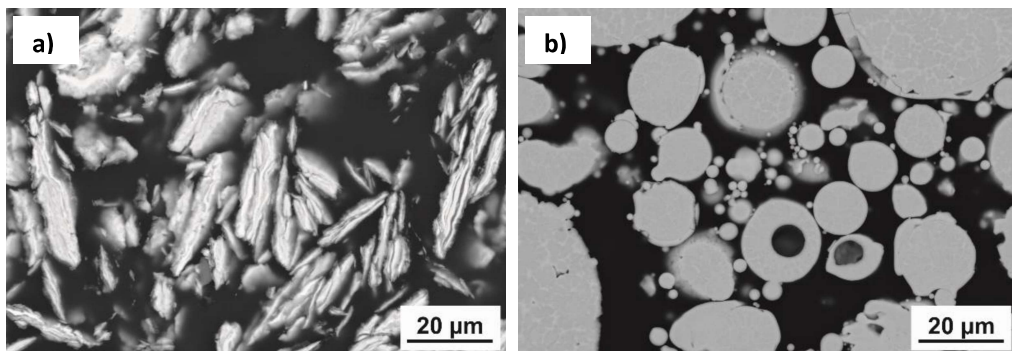


**Figure 1.** SEM (BSD) images of: a) HEM powder and b) atomized powder.

The HEM powder consists of plate-like particles with a heterogeneous structure. Within particles, lamella can be distinguished. The contrast in BSD images indicates that the particles do not have a chemically homogeneous composition.

In contrast, the cross section of atomized powder shows spherical particles and a more homogeneous microstructure. Several phases can be distinguished within particles. This microstructure is in accordance with earlier work on bulk samples [6, 15]. In a next step, the overall chemical composition has been analyzed by EDX. The results, in comparison with the nominal composition, are shown in table 4.

**Table 4.** Chemical composition of HEM and atomized powder measured by EDX.

	Al (at.%)	Co (at.%)	Cr (at.%)	Fe (at.%)	Ni (at.%)	Ti (at.%)
<i>nominal</i>	16.7	16.7	16.7	16.7	16.7	16.7
HEM powder	24.3	19.8	15.7	13.7	13.8	12.7
atomized powder	18.3	16.0	16.9	16.7	16.1	16.0

The chemical composition of the HEM powder deviates from the nominal composition. Especially the content of Al and Ti shows strong deviation. The chemical analysis might be influenced by the inhomogeneous state of powder. In contrast, the composition of the atomized powder is in good accordance with nominal composition. Only the Al content shows a deviation which exceeds 1 at.%. The particle size distribution of all applied feedstock materials was investigated by laser diffraction analysis. The results are displayed in figure 2.

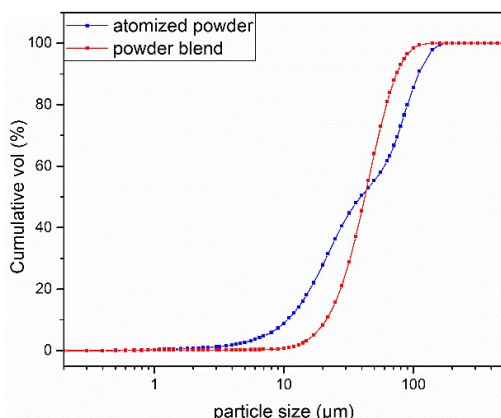


**Figure 2.** Cumulative particle size distribution of powder blend and atomized powder feedstock.

Due to the irregular particle shape of HEM powder, an analysis by laser diffraction was not possible. The evaluation of particle size analysis reveals a  $d_{50}$  value of 41.3  $\mu\text{m}$  and a  $d_{90}$  value of 75.0  $\mu\text{m}$  for the powder blend. In comparison, the atomized powder shows a coarser size distribution with a  $d_{50}$  value of 42.9  $\mu\text{m}$  and  $d_{90}$  value of 109.9  $\mu\text{m}$ . Phase analysis was carried out by XRD. Resulting diffractograms are shown in figure 3.

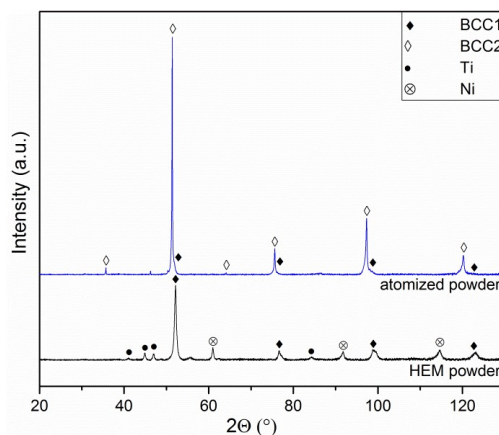


**Figure 3.** XRD patterns of HEM and atomized powder.

The XRD pattern of the HEM powder exhibits minor peaks of elemental Ti and Ni. Consequently, no homogeneous and fully alloyed powder was obtained. These peaks indicate the existence of unmilled Ni and Ti particles. However, a BCC structure (PDF 00-006-0694 / Im-3m (229)) is formed, which is denoted as BCC1.

The diffractogram of the atomized powder displays peaks, which can be ascribed to another BCC phase (PDF 03-065-4198 / Pm-3m (221)) labeled as BCC2. The high intensity diffraction peaks exhibit a shoulder towards higher diffraction angles, indicating the overlapping of diffraction peaks ascribed to the BCC1 phase. Furthermore, powder of the same lot with a coarser powder size distribution has been investigated. Diffraction patterns of this powder clearly reveal peaks, which can be ascribed to the BCC1 phase. Microstructural investigations also show a multiphase structure indicating the existence of the BCC1 phase.

### 3.2 Coating characterization

The first step of coating characterization was the preparation of metallographic cross sections and investigation in SEM. Metallographic cross sections of coatings produced with powder blend, HEM powder and atomized powder feedstock are displayed in figure 4.

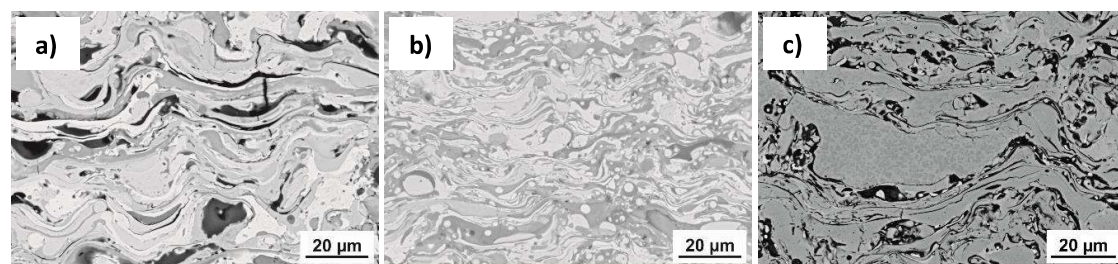


**Figure 4.** SEM (BSD) images of coating cross sections deposited with APS of: a) powder blend, b) HEM powder and c) atomized powder.

The coating type produced with powder blend feedstock exhibits a lamellar and heterogeneous microstructure. Distinct contrast between single lamella can be observed, which indicates strong deviation of local chemical composition. Furthermore, dark oxide lamella exist, which are a result of high temperatures during the APS process and contact of molten powder particles with ambient air.

For the coating deposited with HEM powder, a similar microstructure is revealed. However, this coating type shows much smaller phases and no distinct black oxide lamella. Some round particles can be seen in the coating, which are a result of incomplete particle melting and mixing during coating process.

In the last coating type, deposited with atomized powder, no distinct contrast can be observed between single lamella, indicating a more homogeneous microstructure. However, there is visible contrast within single lamella, which suggests that several phases exist. Furthermore, oxide lamella and pores exist. The overall composition of all coatings has been analyzed by EDX and is displayed in table 5.

**Table 5.** Chemical composition of coatings produced with different feedstock material measured by EDX.

feedstock	Al (at.%)	Co (at.%)	Cr (at.%)	Fe (at.%)	Ni (at.%)	Ti (at.%)
<i>nominal</i>	16.7	16.7	16.7	16.7	16.7	16.7
powder blend	28.5	14.5	15.2	14.7	12.0	15.0
HEM powder	16.1	16.9	11.2	16.1	16.9	22.8
atomized powder	18.7	16.3	15.2	16.3	16.5	17.0

For the coating type produced with powder blend feedstock, a distinct deviation between measured and nominal composition occurs. Especially the Al content differs from the nominal composition. The difference might be caused by vaporization during the coating process as well as the inhomogeneous state of the coating. Coatings produced with HEM powder show a distinctly changed chemical composition especially for Cr and Ti content. In contrast the coating type deposited with atomized powder is in better accordance with the nominal composition. Only the Cr and Ti contents are changed markedly in comparison with the feedstock material (table 4). The smaller deviation in comparison with the two other feedstock materials is probably an effect of the more homogeneous powder microstructure. The powder is already in an alloyed state, which avoids vaporization of single elements. Phase analysis by XRD has been carried out for all coatings. Resulting diffractograms are depicted in figure 5.

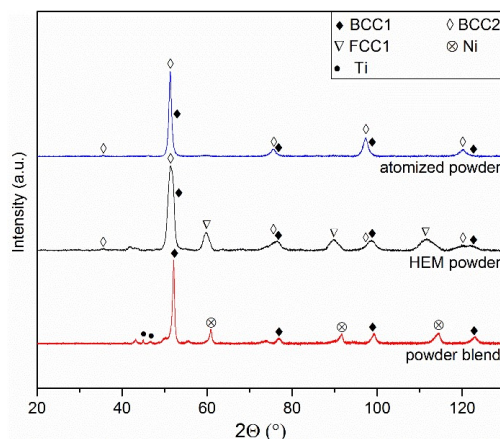


**Figure 5.** XRD patterns of coatings produced with powder blend, HEM powder and atomized powder feedstock.

For the coating type produced by APS of powder blend feedstock, diffraction peaks, which can be referred to several phases appear. A BCC structure (PDF 00-006-0694 / Im-3m (229)), which is denoted as BCC1, is formed. Furthermore, diffraction peaks of pure Ni and Ti appear, showing that no complete alloy formation has occurred during the thermal spray process. The short processing time does not allow for these particles to fully melt and mix with other elements.

The coating type deposited by applying HEM powder exhibits major peaks which can be ascribed to another BCC phase (PDF 03-065-4198 / Pm-3m (221)), labeled as BCC2. Furthermore, diffraction peaks of the BCC1 phase appear. Unlike the diffraction pattern of the HEM powder feedstock (figure 3) no diffraction peaks of pure Ni and Ti emerge, showing that a more homogeneous state is reached after the thermal spray process. Further diffraction peaks can be ascribed to a FCC phase (PDF 01-071-7594 / Fm-3m (225)) named FCC1. For the coatings produced with powder blend and HEM powder feedstock, several small diffraction peaks appear which cannot be ascribed. These diffraction peaks are possibly a result of oxide formation during the thermal spray process.

In comparison with atomized powder feedstock, the diffractogram of the coating type deposited with this powder displays the same major peaks. The peaks can be attributed to the BCC2 phase. According to the diffraction pattern of atomized powder, diffraction peaks exhibit a shoulder towards higher diffraction angles, indicating the overlapping of diffraction peaks ascribed to the BCC1 phase. The investigation of metallographic cross sections (figure 4) reveals a multiphase structure, which also suggests the existence of the BCC1 phase. Hardness HV0.1 was measured in cross sections of all coatings. The results are displayed in figure 6.

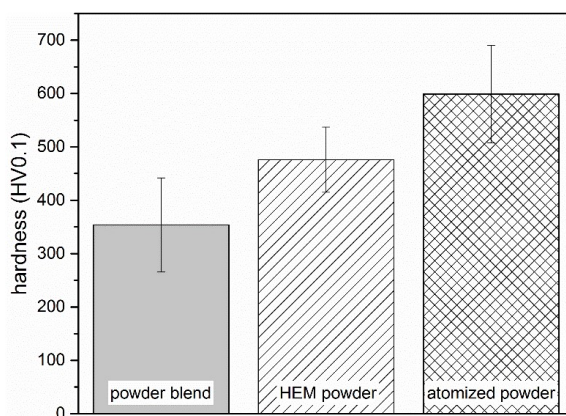


**Figure 6.** Hardness of APS-coatings, produced with different feedstock material.

For the coating type deposited with powder blend feedstock, an average hardness of 354 HV0.1 was measured. The coating type produced with HEM powder has an increased average hardness of 476 HV0.1, which is probably caused by the finer microstructure and the absence of pure Ni and Ti (XRD / figure 5). Both coatings show a strong standard deviation of over 10 %, which is caused by the inhomogeneous microstructure of the coatings. For the coating type deposited with atomized powder, an average hardness of 599 HV0.1 was measured. The results of wear tests under different tribological conditions are displayed in figure 7.

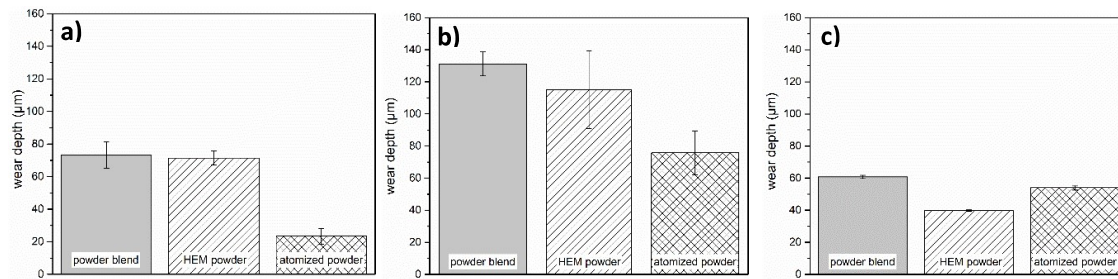


**Figure 7.** Measured resulting wear depth of coatings in: a) ball-on-disk wear, b) oscillating wear and c) scratch test.

The results of the ball-on-disk wear test only show minor difference in wear depth of coatings deposited with powder blend and HEM powder feedstock, indicating a similar wear resistance. In contrast, the coating type produced with atomized powder reveals a distinctly reduced wear depth and thus improved wear resistance.

The evaluation of the oscillating wear test shows that the highest wear depth and lowest wear resistance was achieved for the coating type deposited with powder blend feedstock. For the coating type produced with HEM powder, the wear depth is slightly reduced. However, this coating type exhibits the highest standard deviation, which elucidates the inhomogeneous state of this coating type. For the coating type deposited with atomized powder the wear depth is clearly reduced, which is caused by the fully alloyed state and a more homogeneous microstructure. Furthermore, this coating type exhibits the highest hardness, which is beneficial at the present wear mechanism.

The progressive mode scratch test has been analyzed by determining the maximum wear depth of the scratches. The highest wear depth was measured for the coating type deposited with powder blend feedstock. In comparison, a slightly reduced wear depth and increased wear resistance was determined for the HEM powder coating. No further decrease of wear depth could be achieved for the coating type deposited with atomized powder. The resulting wear resistance in the scratch test is in between the coatings produced with powder blend and HEM powder. Due to the deviation of wear behavior in the scratch test compared to ball-on-disk and oscillating wear tests, all scratches were investigated by optical microscopy. Figure 8 shows the scratch area where the maximum load was applied in the progressive mode scratch test.

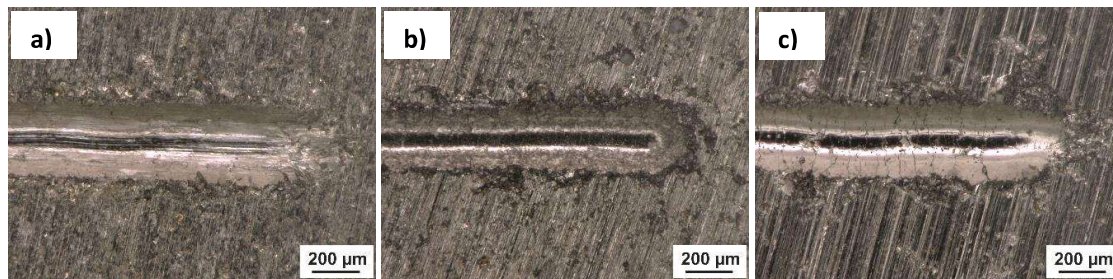


**Figure 8.** Surface of coatings produced with a) powder blend, b) HEM powder and c) atomized powder feedstock after progressive mode scratch test.

The scratches in the coatings produced with powder blend and HEM powder feedstock show a relatively smooth surface with only small spalling of material at the edge of the scratch. In contrast, the coating type produced with atomized powder shows distinct cracks on the bottom of the scratches. Furthermore, a spalling of material at the edge is visible. The increase of measured maximum wear depth and the appearance of cracks in the scratch test under abrasive wear stress indicates the brittle behavior of this coating type.

#### 4. Conclusion

The applicability of the equimolar CCA AlCoCrFeNiTi for surface engineering has been analyzed in this study. Three different feedstock materials (powder blend, HEM and atomized powder) were investigated regarding their suitability to be deposited by APS. The investigation of different feedstock materials reveals that inert gas atomization is most suitable to produce homogeneous and spherical alloyed powder. Two BCC solid solutions are formed for this production method. According to earlier investigations on bulk material, a multiphase structure appears. Furthermore, APS coatings were produced for all feedstock materials. For the coatings produced with powder blend and HEM powder feedstock, a heterogeneous microstructure is formed. By applying atomized powder, a more homogeneous microstructure occurs. Within the coatings, several phases can be distinguished. For the coatings produced by applying atomized powder feedstock the same BCC solid solutions like in the feedstock material are formed. However, oxide lamella and pores exist, which might be reduced by further optimization of coating parameters. Furthermore, the application of other thermal spray technologies with lower heat input like high-velocity-oxygen-fuel spraying has to be investigated. The investigation of wear behavior revealed best wear resistance in ball-on-disk and oscillating wear test for the coatings deposited with atomized powder due to the more homogeneous microstructure. In the scratch test, a slightly lower wear resistance compared to the HEM powder coatings is observed. Furthermore, cracks appear for the coatings produced with atomized powder feedstock, indicating brittle behavior.

#### Acknowledgements

The authors gratefully acknowledge the Arbeitsgemeinschaft Industrieller Forschungsvereinigungen "Otto von Guericke" e.V. (AiF) for support of this work (AiF-No. KF2152612CK4) with funds from the German Federal Ministry for Economic Affairs and Energy. The authors thank Marc Pügner for conducting the XRD measurements and assistance during their evaluation and Ilka Günther for conducting the particle size analysis.

#### References

- [1] Yeh J-W, Chen S-K, Gan J-Y, Lin S-J, Chin T-T, Shun T-T, Tsau C-H and Chang S-Y 2004 *Metall. Mater. Trans. A* **35** 2533-2536
- [2] Yeh J-W, Chen Y-L, Lin S-J and Chen S-K 2007 *Mater. Sci. Forum* **560** 1-9
- [3] Cantor B, Chang I T H, Knight P and Vincent A J B 2004 *Mater. Sci. Eng. A* **375-377** 213-218
- [4] Murty B S, Yeh J-W and Ranganathan S 2014 *High-Entropy Alloys* (Elsevier Inc.)
- [5] Miracle D B, Miller J D, Senkov O N, Woodward C, Uchic M D and Tiley J 2014 *Entropy* **16** 494-525
- [6] Zhou Y J, Zhang Y, Wang Y L and Chen G L 2007 *Appl. Phys. Lett.* **90** 181904
- [7] Wang Y, Ma S, Chen X, Shi J, Zhang Y and Qiao J 2013 *Acta Metall. Sin (Eng. Lett.)* **26/3** 277-284
- [8] Yu Y, Wang J, Li J, Kou H and Liu W 2015 *Mater. Lett.* **138** 78-80
- [9] Zhang K and Fu Z 2014 *Intermetallics* **22** 24-32
- [10] Chuang M-H, Tsai M-H, Wang W-R, Lin S-J and Yeh J-W 2011 *Acta Mater.* **59** 6308-6317
- [11] Yu Y, Liu W M, Zhang T B, Li J S, Wang J, Kou H C and Li J 2014 *Metall. Mater. Trans. A* **45** 201-207
- [12] Ang A S M, Berndt C C, Sesso M L, Anupam A, Praveen S, Kottada R S and Murty B S 2014 *Metall. Mater. Trans. A* **46** 791-800
- [13] Wang L M, Chen C C, Yeh J-W and Ke S T 2011 *Mater. Chem. Phys.* **126** 880-885
- [14] Huang P-K, Yeh J-W, Shun T-T and Chen S-K 2004 *Adv Eng Mater* **6** 74-78
- [15] Soare V, Mitrica D, Constantin I, Badilita V, Stoiciu F, Popescu A-M J and Carcea I 2015 *J. Mater. Sci. Technol.* **31** 1194-1200